Performance evaluation of modified tuned liquid dampers for seismic response control of nonlinear benchmark buildings

A.H. Daneshmand and A. Karamodin*

Department of Civil Engineering, Ferdowsi University of Mashhad, Mashhad, Iran.

Abstract. In this study, the performance of Modified Tuned Liquid Damper (MTLD) is evaluated to control the seismic response of 9- and 20-story nonlinear benchmark buildings. MTLD is a type of Tuned Liquid Damper (TLD) that is equipped with a rotational spring at the base and thus experiences both horizontal and rotational motion with structural vibration. The equations obtained by shallow water wave theory are used to describe the water sloshing in the MTLD tank. The optimal design of main MTLD parameters such as dimensionless rotational stiffness, mass and frequency ratio, and the tank distance from the top of the structure are investigated. In addition, the effects of far-field and near-field earthquakes on MTLD performance are discussed and compared with the performance of TLD in detail. The results show that MTLD is somewhat more efficient than TLD both in reducing seismic response and reducing structural damage caused by nonlinear behavior of the structures.

1. Introduction

The interest of using supplemental damping devices for control of structures has increased over the past decades. Tuned Liquid Dampers (TLDs) are one of these supplemental passive devices. Liquid sloshing in these devices causes energy dissipation through wave breaking, boundary layer friction and free-surface contamination [1]. If the water height to tank length ratio is less than 0.15, they are called shallow and otherwise deep tanks. This classification is based on shallow water wave theory in coastal engineering [2]. In the shallow type, damping and energy dissipation are more likely because almost all of the liquid mass contributes to the vibrations. Also, Water sloshing behavior is nonlinear, and wave breaking occurs under severe excitations [3].

The implementation of TLDs to reduce structural vibrations was first proposed by Bauer [4]. In order to model water sloshing inside the TLD, several types of equivalent mechanical and mathematical models have

*. Corresponding author.
E-mail address: a-karam@um.ac.ir (A. Karamodin)
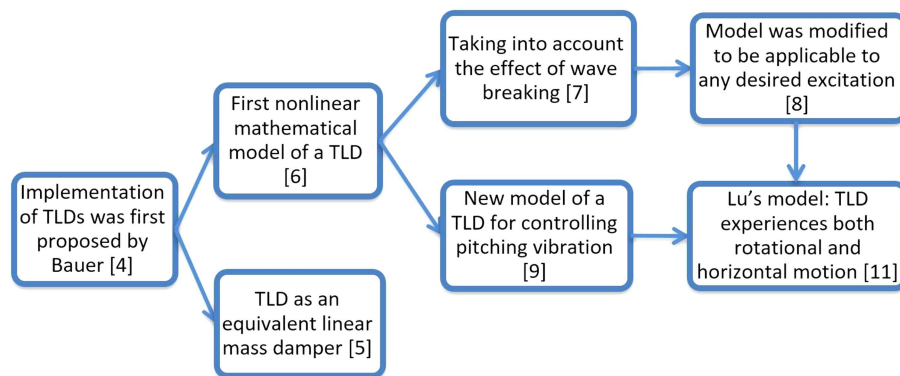
Figure 1. Review of the evolution of the mathematical model of fluid vibration in the TLD.

been introduced. Kareem and Sun [5] first modeled liquid dampers as an equivalent linear mass damper. The first nonlinear model of a rectangular TLD was developed by Shimizu and Hayama [6], in which the shallow water wave theory is combined with potential flow theory. Sun et al. [7] extended the same model by taking into account the effect of wave breaking on damping and TLD frequency. The Sun model was modified by Koh et al. [8] to be applicable to any desired excitation. Based on the nonlinear shallow water wave theory, the effectiveness of TLD for controlling pitching vibration was studied by Sun et al. [9]. The study by Banerji et al. [10] on TLD for controlling different vibrations using the Sun model showed that there is a discrepancy between the analytical and experimental results due to ignoring the wave breaking effect. Lu et al. [11] proposed a new numerical model to simulate water sloshing inside a rectangular TLD that experiences a combination of rotational and horizontal motion. in Lu's model, the shallow water theory is applied with an improved boundary shear model to accommodate for the part of the TLD floor exposed to air by large excitations (brief review of the evolution of the mathematical model of fluid vibration in the TLD is shown in Figure 1). Implementation of the Lu model by Samantha and Banerji [12] showed that under large-scale harmonic excitations, this model predicts the sloshing of water inside the TLD better than Sun's model. In the last few years, many strategies have been investigated to increase TLD efficiency, such as the semi-active structure-multiple TLD systems [13], combined TLD with lead-rubber bearing systems or Tuned Mass Damper (TMD) [14,15], use of rotatable baffles or incompressible smoothed particles inside the tank [16,17], TLDs with sloped bottom [18,19], and TLD with floating base or roof [20,21].

Samantha and Banerji [22] introduced the Modified Tuned Liquid Damper (MTLD) using the Lu model to control structural vibrations. The MTLD is a TLD that equipped with a rotational system consisting of a set of springs and pivot at the base

and attached to the top of the structure. Chang et al. [23] studied the application of MTLD to control a single-degree-of-freedom structure under harmonic excitation and ground motion records, analytically and experimentally. Their study showed that when MTLD is optimally designed, it is more effective in controlling the structure than the TLD. More recently, Kamgar et al. [24] investigated the efficacy of MTLD in seismic protection of buildings with linear behavior considering the effect of soil-structure interaction, and concluded that MTLD decreased maximum structural responses efficiently.

A number of studies have also evaluated the performance of TLD on multiple-degree-of-freedom structures. Among them, one can note the study of the application of deep TLD on structures using Real-Time Hybrid Simulation (RTHS) method by Wang et al. [25], the numerical and empirical evaluation of TLD performance by Eswaran et al. [26], and analysis the effectiveness of TLD in controlling the vibration of high rise building by Tuong et al. [27]. As far as the authors know the effect of MTLD on building responses and damage criteria in nonlinear multiple-degree-of-freedom structures has not been studied. In this study, the best performance of passive MTLD for controlling 9- and 20-story nonlinear benchmark building structures introduced by Ohtori et al. [28] has been investigated under the excitation of four far and near-field earthquake records with varying intensities (totally 10 records). Afterwards, by increasing the rotational stiffness of MTLD and converting it to TLD, the same study was again performed and the results were compared. Herein, it is also attempted to design MTLD parameters to optimally reduce the maximum drift criterion.

2. Analytical model for MTLD

2.1. Governing equations
A TLD with rigid rectangular tank is shown in Figure 2. The length and width of the tank are determined
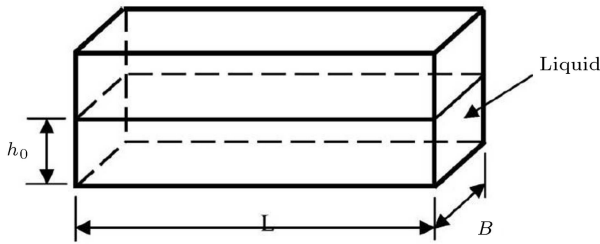
**Figure 2.** Schematic diagram of TLD [22].
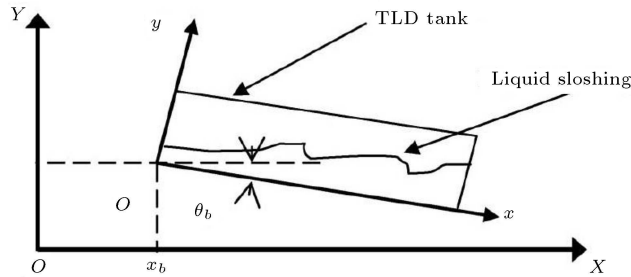
Figure 3. TLD under both horizontal and rotational motions [22].

by L and B, respectively, and the initial depth of water inside the tank is shown by h_0.

A model of the tank affected by both horizontal and rotational motions is shown in Figure 3. x_b and θ_b represent the horizontal and rotational motions of the tank, respectively. It should be noted that x_b represents absolute displacement above the structure and θ_b represents clockwise rotation [22].

The water pressure is assumed to be hydrostatic, the velocity profile at the vertical cross-section is uniform, and the water height does not reach the top of the tank during sloshing. To support these hypotheses, rotational motion (θ_b) must be small. Lu et al. [11] suggested that the value of θ_b be limited to $10°$. According to the above assumptions, and based on shallow water wave theory, the governing equations of the water sloshing motion, in terms of mass and momentum survival principles are as follows [11]:

$$\frac{\partial h}{\partial t} + h\frac{\partial V}{\partial x} + V\frac{\partial h}{\partial x} = 0, \tag{1}$$

$$\frac{\partial V}{\partial t} + V\frac{\partial V}{\partial x} + g\frac{\partial h}{\partial x} - g(\theta_B - S) + \frac{\partial^2 x_B}{\partial t^2} = 0. \tag{2}$$

Assuming the liquid to be at rest at $t = 0$, the initial and boundary conditions for solving Eqs. (1) and (2) are given in Eqs. (3) and (4), respectively:

$$V\,|_{x=0} = V\,|_{x=L} = 0, \tag{3}$$

$$h\,|_{t=0} = h_0 \quad \text{and} \quad V\,|_{t=0} = 0 \qquad \forall x \in [0, L]. \tag{4}$$

In Eqs. (1)–(4) S represents slope of the energy grade line, gth gravitational acceleration, Vth velocity of

water relative to the tank floor and hth sloshing water depth at location x and time t. By solving the governing Eqs. (1) and (2), water sloshing height is obtained. Afterwards, considering the hydrostatic pressure of water, the sloshing force applied to the rectangular tank walls (F) and the moment on the tank base (M) can be obtained from the following equations [9]:

$$F = -\frac{1}{2}\rho g B\left(h_R^2 - h_L^2\right), \tag{5}$$

$$M = -\frac{1}{6}\rho B a_y\left(h_R^3 - h_L^3\right) - \int_0^L \rho B a_y hx\,dx, \tag{6}$$

where h_R and h_L represent the water height at the end of right and left tank walls, respectively. In Eq. (6), the first part shows the moment caused by the horizontal forces acting on the two end walls of the tank relative to the tank floor, and the second part deals with the moment caused by the vertical forces of the water relative to the tank floor. Also, a_y is the vertical acceleration of water in the tank, calculated from the following equation [9]:

$$a_y \approx -g\cos\theta - \ddot{z}_0\cos\theta - \ddot{\theta}x + \ddot{x}_0\sin\theta. \tag{7}$$

Herein, $\ddot{z}_0$ and $\ddot{x}_0$ represent centrifugal and tangential accelerations, respectively.

2.2. Solution method
The governing equations of MTLD are numerically solved with the Lax Finite Scheme [29]. A detailed discussion of the solution process can be found in the literature Lu et al. [11]. The minimum number of suitable segment lengths (η) for the analysis of water sloshing is calculated from the relation proposed by Shimizu and Hayama [6]:

$$\eta = \frac{\pi}{2arc\cos\left(\sqrt{\frac{\tanh(\pi\varepsilon)}{2\tanh\left(\frac{\pi\varepsilon}{2}\right)}}\right)}, \qquad \left(\varepsilon = \frac{h_0}{\left(\frac{L}{2}\right)}\right). \tag{8}$$

To obtain a stable numerical solution, Lu et al. [11] have restricted the maximum time step (Δt) to the following result:

$$\Delta t \leq \frac{\Delta x}{\max\left(|V| + \sqrt{gh}\right)}. \tag{9}$$

2.3. Structure-MTLD equations of motion
The basic model of a Single Degree of Freedom (SDOF) system equipped with MTLD presented by Samantha and Banerji [22] is shown in Figure 4(a). As can be seen, the tank is connected to SDOF using a rigid rod and a rotational spring. One end of the rigid rod is connected rigidly to the tank and the other end is connected to SDOF by a rotational spring. The
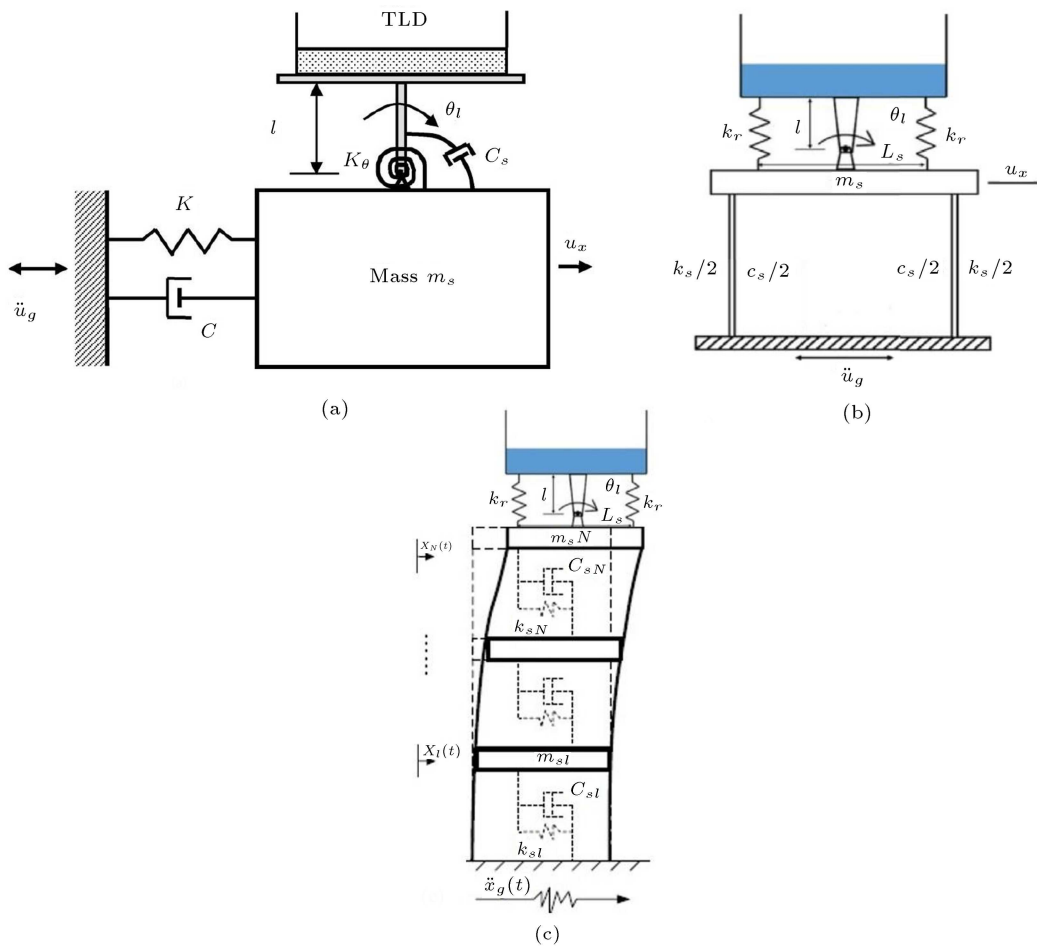
Figure 4. (a) Schematic diagram of a shear-beam structure with an idealized MTLD [22], (b) Schematic of a single frame with a practical MTLD [23] and (c) MDOF structure-MTLD system.

practical installation of MTLD on top of a SDOF structure is shown in Figure 4(b) [23]. In this model, the rotational spring with stiffness k_θ is replaced by two linear springs with stiffness k_r and distance L_s which are easily related by the following relation [23]:

$$k_\theta = \frac{k_r L_s^2}{2}. \tag{10}$$

Figure 4(c) represents the multiple degree of freedom structure (MDOF) equipped with MTLD system. Since an MTLD has also a rotational degree of freedom in addition to horizontal degree of freedom of the traditional TLD, and given the equation of motion presented for SDOF with MTLD by Samantha and Banerji [22], the equation of motion of MTLD-controlled N degree of freedom structure obtained by Formula (11) is shown in Box I, where m_{si}, c_{si}, and k_{si} represent the components of the mass, damping, and stiffness matrices, respectively. m_t represents the total lumped mass of MTLD and l indicates the rod length (tank floor height from the structure top). j_1 and j_2 indicates the mass moment inertia of the rod and tank, respectively. c_θ is the damping coefficient of the

rotational spring system. In addition, $\ddot{u}_{xi}$, $\dot{u}_{xi}$, and u_{xi} represent the components of the acceleration, velocity, and relative displacement vectors of the structure stories, respectively. Similarly, $\ddot{\theta}_l$, $\dot{\theta}_l$, and θ_l represent the rotational acceleration, velocity, and angle of rotation of the tank relative to the vertical axis, respectively.

3. Benchmark buildings and design of MTLDs

In this paper, the nonlinear 9 and 20 story benchmark building structures defined by Ohtori et al. [28] are considered for numerical investigation. Building's lateral load-resisting system includes steel perimeter Moment-Resisting Frames (MRFs) with simple interior frames. In the nonlinear evaluation of benchmark structures, a bilinear hysteresis model is used to model the plastic hinges at the end of the moment-resistant elements. The total seismic mass on the ground surface of the 9 and 20 story benchmark structures is 9×10^6 and 1.11×10^7 kg, respectively. details and mathematical modeling of benchmark structures are available in Ohtori et al. [28]. The plan and a perimeter frame, together with the structural properties of the 9-story

$$
\begin{bmatrix}
m_{s1} & 0 & \cdots & & 0 \\
0 & \ddots & & & \vdots \\
\vdots & & m_{sN}+m_t & m_t \\
0 & \cdots & m_t & m_t+\frac{j_1+j_2}{l^2}
\end{bmatrix}
\begin{bmatrix}
\ddot{u}_{x1} \\
\vdots \\
\ddot{u}_{xN} \\
l.\ddot{\theta}_l
\end{bmatrix}
+
\begin{bmatrix}
[c_s]_{N \times N} & [0]_{N \times 1} \\
[0]_{1 \times N} & \frac{c_\theta}{l^2}
\end{bmatrix}
\begin{bmatrix}
[\dot{u}_x]_{N \times 1} \\
l.\dot{\theta}_l
\end{bmatrix}
+
$$

$$
\begin{bmatrix}
[k_s]_{N \times N} & [0]_{N \times 1} \\
[0]_{1 \times N} & \frac{k_\theta}{l^2}
\end{bmatrix}
\begin{bmatrix}
[u_x]_{N \times 1} \\
l.\theta_l
\end{bmatrix}
=
\begin{bmatrix}
-\ddot{u}_g m_{s1} \\
\vdots \\
F-\ddot{u}_g(m_{sN}+m_t) \\
F+\frac{M}{l}-\ddot{u}_g m_t
\end{bmatrix}.
\tag{11}
$$

Box I
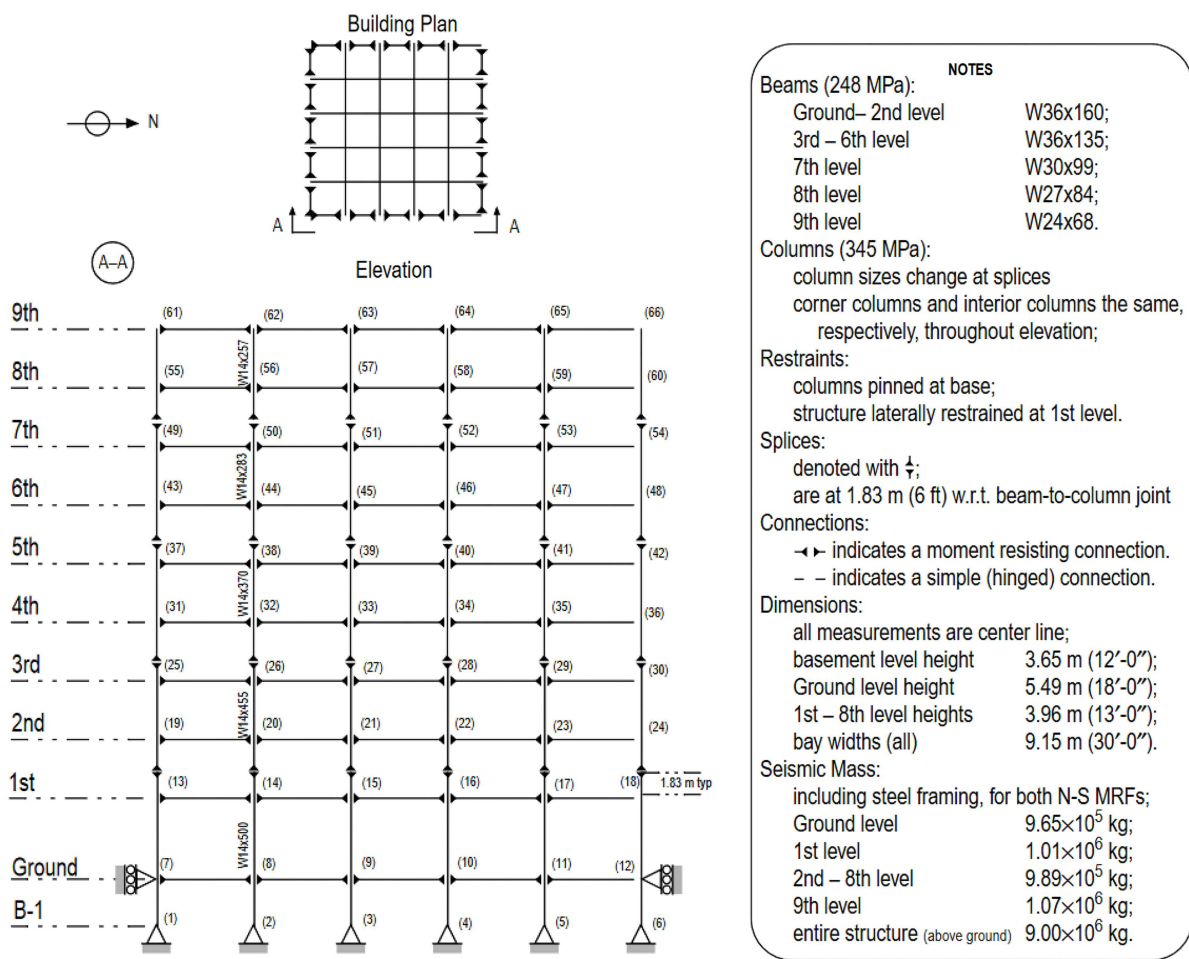
Figure 5. Nine-story benchmark building [28].

benchmark building are shown in Figure 5. Modeling of benchmark buildings equipped with MTLD have been conducted in MATLAB and the governing equations of motion have been solved by a MATLAB code developed by Ohtori et al. [28] for benchmark buildings.

Since, equations governing fluid sloshing motion are determined based on shallow water wave theory, it is therefore necessary to consider the ratio of initial water depth to tank length $\left(\frac{h_0}{L}\right)$ equal to or lower than 0.15 [10]. Hence, in the design of TLDs, this ratio is set to 0.15.

The frequency of the liquid damper is calculated according to the following equation [30]:

$$
f_w = \frac{1}{2\pi} \sqrt{\frac{\pi g}{L} \tanh\left(\frac{\pi h_0}{L}\right)}.
\tag{12}
$$

Frequency ratio (α) represents the ratio of struc-

Table 1. The characteristics of the optimally designed MTLDs for each benchmark story.

Benchmark structure	Dimensions (m)	h_0 (m)	f_w (HZ)	ξ_θ	α	l (m)
9- Sstory	$L = 1.117$, $B = 19.985$	0.168	0.554	0.5%	0.8	2
20- story	$L = 3.220$, $B = 17.835$	0.483	0.326	0.5%	0.8	2

ture's natural frequency (f_s) to sloshing frequency of liquid damper (f_w). The frequency ratio (α) as will be described in Section 4.2 is set to 0.8 for both structures. The natural frequency of the first mode of the 9 and 20 story benchmark structures is 0.443 and 0.261 Hz, respectively. So, the sloshing frequency of the TLDs (f_w) was obtained to be 0.554 and 0.326 Hz, respectively. According to $\frac{h_0}{L} = 0.15$, the length of MTLD tanks mounted on 9- and 20-story benchmark structures, using Eq. (12), was determined to be 1.117 and 3.22 m, respectively. So, the initial water depth within the MTLD tanks for controlling 9- and 20-story benchmark structures is calculated as 0.168 and 0.483 m, respectively (see Table 1).

By determining h_0 and L for the modified liquid dampers, their widths are determined in relation to mass ratio. The mass ratio (μ) is defined as the ratio of the liquid damper mass (m_w) to the structure's seismic mass (m_s). Since MTLDs are designed only for one N-S seismic frame of benchmark structures, the MTLD mass (m_w) is determined based on half the structure's total seismic mass (m_s). By considering use of several MTLDs with similar properties that work in parallel, width of MTLD tank for 9- and 20-floor benchmark structures at all mass ratios is 19.985 and 17.835 m, respectively (see Table 1). So, for controlling the 20-story benchmark structure at 3, 2, 1 and 0.5% mass ratios, 6, 4, 2 and 1 MTLDs, and for controlling the 9-story benchmark structure at the same mass ratios 36, 24, 12 and 6 MTLDs are needed, respectively.

The inherent damping of liquid dampers caused by the tank walls and floor, is calculated as follows [13]:

$$\xi_{TLD} = \frac{1}{2\pi} \sqrt{\frac{\vartheta_w}{\pi f_w}} \left(1 + \frac{h_0}{B}\right), \tag{13}$$

where ϑ_w is the kinetic viscosity of water (1.002×10^{-6}). According to the specifications of designed MTLDs, the damping of each damper for the 9- and 20-story benchmark structures is 0.012 and 0.016%, respectively. which are very low.

In order for MTLD to perform best in structural control, it is necessary to optimally select the rotational spring stiffness. Investigation on the optimum stiffness of MTLD rotational springs is performed using Dimensionless Rotational Stiffness Parameter (DRSP), introduced by Samantha and Banerji [22]:

$$\gamma = DRSP = \frac{k_\theta}{K_s l^2}. \tag{14}$$

where, K_s is the equivalent stiffness of the structure's first mode. Considering the first structural mode frequency (f_s) as the dominant frequency and assuming that the frequency ratio (α) remains constant during the vibration of the structure, it is expected that when the frequency of the MTLD rotating system (f_θ) equals the water sloshing frequency (f_w), we will approximately have the best MTLD performance in controlling the structure:

$$f_w = f_\theta = \sqrt{\frac{k_\theta}{m_w l^2}}. \tag{15}$$

Therefore, according to the Eq. (14) regarding that $\alpha = \frac{f_s}{f_w}$ and $\mu = \frac{m_w}{m_s}$, the following approximate relation can be reached for optimum γ:

$$\gamma_{opt} = \frac{\mu}{\alpha^2}. \tag{16}$$

By replacing above γ_{opt} in Eq. (14), it is possible to approximately determine the required optimum rotational stiffness of the passive MTLD. However, the values of γ_{opt} are also evaluated numerically (with consistently change rotational spring stiffness) for each case.

4. Numerical study

4.1. Performance criteria

In this study, nonlinear time history analysis was performed to evaluate the effectiveness of MTLD in reducing the seismic response of the two benchmark structures. Two far-field earthquakes (El Centro and Hachinohe) and two near-field earthquakes (Northridge and Kobe) with different levels have been used for this purpose. The Peak Ground Acceleration (PGA) of these earthquakes are 3.417, 2.25, 8.267, and 8.178 m/sec² respectively [28]. In addition, different levels of each earthquake record were used, including: 0.5, 1, and 1.5 times the magnitude of El Centro and Hachinohe and 5.0 and 1 times the magnitude of Northridge and Kobe.

The number of suitable segment lengths (η) for the analysis of water sloshing of the MTLD tank located on the 9- and 20-story structures is considered to be 20 and 50, respectively. A time step of 0.001 s was also used to ensure the Eq. (9) is satisfied, as well as increasing the accuracy and convergence of the

solution. Ten important performance criteria specified by Ohtori et al. [28]. These criteria include: peak inter-story drift ratio (J_1), maximum acceleration level (J_2), maximum base shear (J_3), normed inter-story drift ratio (J_4), normed level acceleration (J_5), normed base shear (J_6), Ductility factor (J_7), dissipated energy at the end of members (J_8), ratio of plastic hinges sustained by structure (J_9) and normed ductility factor (J_{10}). Among the mentioned criteria, five criteria are used in this study, these criteria are divided into two categories. The first category is formulated based on building responses and includes two criteria: J_1 and J_2. The second set of performance criteria relates to the nonlinear behavior of structures and discusses structural damage. This category includes three criteria of J_7 to J_9.

4.2. The effect of frequency ratio (α) and rod length (l)

The main purpose of this study is to investigate the effect of MTLD on reducing maximum structural drift response (J_1 criterion) and its comparison with traditional TLD. It is firstly necessary to select the optimal frequency ratio (α). Then, the effects of rod length (l) on the maximum rotation of TLD (Max. θ_B) are investigated.

In the study by Samantha and Banerji [22] on a SDOF structure with MTLD, it has been suggested that increasing rotational damping up to 0.5% has negligible effect on the responses. Therefore, the inherent damping of the MTLD rotational system (ξ_θ) is considered to be 0.5%. Summary of the effect of frequency ratio (α) on the maximum drift response (J_1) of 9 and 20 story benchmark structures with MTLD for Mass Ratio 3%, under El Centro earthquake is shown in Figure 6. The graph shows maximum drift ratio criterion (J_1) for four different α values equal to 0.75, 0.8, 1 and 1.2 for each of the two benchmark structures. As can be seen in Figure 6, the best drift response for 9-story benchmark structure occurs at α equal to 0.8 and for 20-story benchmark structure at α equal to 0.75. Previously, Chang et al. [23] proposed the best frequency ratio being equal to 0.8 for adjusting MTLD on a SDOF structure. Considering the low difference of α value for 9 and 20 story structures, a frequency ratio of 0.8 was selected to investigate the effect of TLDs on benchmark structures.

Effect of rod length (l) on the maximum MTLD rotation of 9 and 20 story benchmark structures for 3% mass ratio, under El Centro earthquake is shown in Figure 7. according to the results of this figure, it is necessary to consider a 2 m rod length for the MTLD system on 9 and 20 story benchmark structures to reduce the tank rotation to below 10 degrees.

The characteristics of the optimally designed MTLDs are summarized in Table 1.
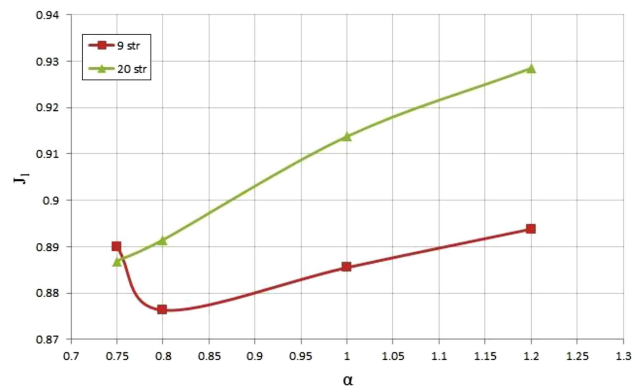
Figure 6. The effect of frequency ratio (α) on the maximum drift response (J_1) of 9- and 20- story benchmark structures with MTLD for Mass Ratio of 3%, under El Centro earthquake.
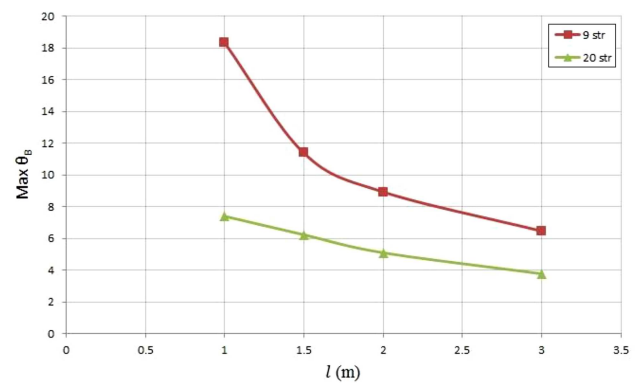
Figure 7. The Effect of rod length (l) on maximum MTLD rotation for 3% mass ratio, under El Centro earthquake.

4.3. Time history comparison of uncontrolled and controlled drifts

Figures 8 and 9 represent the top floor drift time history plots of the 9- and 20-story benchmark TLD and MTLD-controlled structures under 0.5 Kobe and 1 Kobe earthquakes, respectively. Figure 8 shows MTLD has a greater effect on reducing the maximum top floor drift of uncontrolled structure compared to TLD (up to 16%). The same result can be seen in Figure 9 for the 20-story structure.

Figure 10 shows the effect of MTLD on the top floor drift time history of the 9-story benchmark structure under the Northridge earthquake for a mass ratio of 3%. As shown in the diagram, the maximum top floor drift of the 9-story controlled structure after the earthquake peak, increases by approximately 1.5% relative to the earthquake peak, and following the diagram, the top floor drift of the 9-story MTLD-controlled structure becomes greater than that of the uncontrolled 9-story structure. The main reason for this may be mis-tunning of MTLD. Because the MTLD design and its frequency tuning are for linear behavior of the structure while under such a high-intensity and
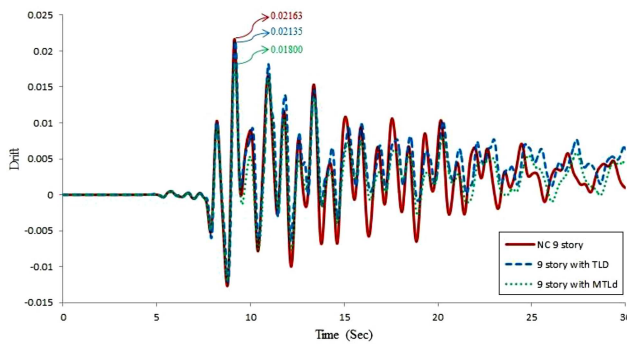
Figure 8. Time histories of top floor drift for the uncontrolled and controlled 9-story benchmark structure under 0.5 Kobe earthquake.
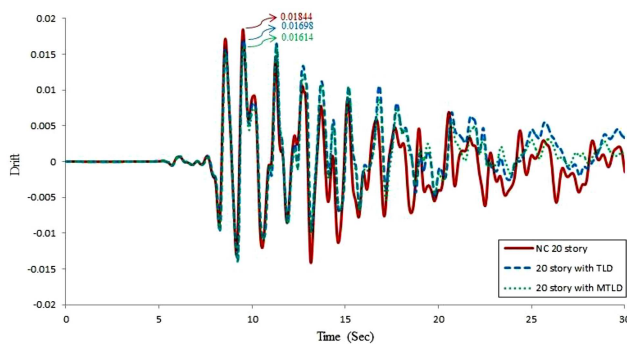
Figure 9. Time histories of top floor drift for the uncontrolled and controlled 20-story benchmark structure under Kobe earthquake.
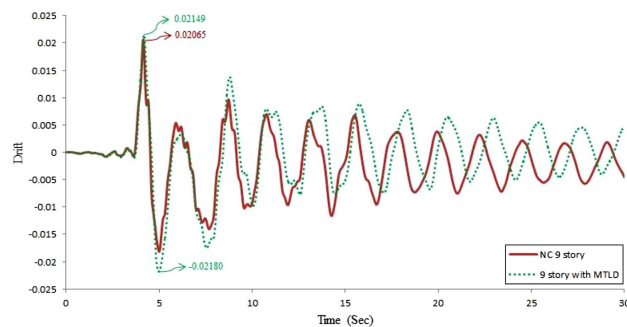
Figure 10. Time histories of top floor drift for the uncontrolled and controlled 9-story benchmark structure under Northridge earthquake.

near-field earthquake, the structural behavior has been be changed to nonlinear and so the period of the structure has been increased. Furthermore, it can be seen in Figure 10, that after the earthquake peak, the period of the structure has been increased.

4.4. Effectiveness of MTLD and comparison with TLD

As the main purpose of this study is to investigate the effect of MTLD on the reduction of maximum drift response, it has been attempted to adjust the dimensionless rotational stiffness parameter (γ) to obtain the best response for the criterion of maximum drift ratio (J_1). However, the results of the effect of MTLD on other criteria are also examined. Mass ratios of 0.5, 1, 2, and 3% are provided for the 9- and 20-story benchmark structures.

The results of the effect of MTLD for the far-field and near-field earthquakes are shown respectively in Tables 2 and 3. In these tables, the optimal dimensionless rotational stiffness parameter (γ_{opt}) for J_1, and five performance criteria at different mass ratios are presented. However, the mean values of the five performance criteria are shown in Table 4 separately for near and far field earthquakes. In order to compare the effect of MTLD with traditional TLD on benchmark structures, the results of Mean decrease of performance criteria responses for MTLD-controlled benchmark structures compared to traditional TLD-controlled ones, are shown in Table 5.

Examining the changes of γ_{opt} to achieve the optimal response of the maximum drift ratio criterion (J_1) in Tables 2 and 3 shows that as expected (according to Eq. (16)), with decreasing mass ratio, the γ_{opt} values decrease. By choosing $\alpha = 0.8$ and using Eq. (16), the expected γ_{opt} values for mass ratios of 0.5, 1, 2, and 3% were equal to 0.008, 0.016, 0.032 and 0.048, respectively. results show that in most cases the γ_{opt} values are close to the γ values obtained from Eq. (16) to achieve the best MTLD performance. However, in some cases it is observed that the γ_{opt} values vary from the γ values obtained by this equation. It must be noted that this equation is developed by the assumption of linear behavior for a SDOF system. So, this alteration can be due to nonlinear behavior and miss adjustment of the frequency ratio under high intensity excitations as well as the participation of higher modes especially, for the 20-story structure.

From Tables 2 and 3, it is generally seen that the effect of MTLD is not the same for all the earthquakes and structures, and largely depends on the characteristics of the ground motions and the structure itself. Since the reduction of maximum drift criterion (J_1) was considered as the main criterion, it can be seen that the maximum reduction of this criterion for the 20-story structure is about 13% under the El Centro and Kobe earthquakes and about 18% for the 9-story structure under 0.5 Kobe earthquake. For the 20-story structure in all earthquakes except the 0.5 Northridge earthquake and for the 9-story structure in all the earthquakes except the Northridge earthquake, the use of MTLD improved the structural structure performance at maximum drift criterion. Variations in the influence of MTLD on the J_1 criterion are not uniform with changes in mass ratios. In many cases such as 20-story benchmark structure under the effect of most earthquakes, maximum drift is also reduced by decreasing the mass ratio. This could be an advantage,

Table 2. Performance criteria responses of the 9- and 20-story benchmark structures with MTLD under far-field earthquakes for mass ratios of 0.5, 1, 2, and 3%.

	20- story benchmark building											
	0.5 El Centro				1 El Centro				1.5 El Centro			
μ	3%	2%	1%	0.5%	3%	2%	1%	0.5%	3%	2%	1%	0.5%
γ_{opt}	0.050	0.033	0.017	0.008	0.052	0.033	0.017	0.008	0.055	0.038	0.019	0.008
J_1	0.91	0.89	0.88	0.87	0.91	0.90	0.88	0.87	0.90	0.90	0.89	0.88
J_2	0.62	0.65	0.73	0.78	0.62	0.65	0.73	0.78	0.64	0.68	0.76	0.81
J_7	0.85	0.88	0.88	0.89	0.85	0.88	0.88	0.89	0.87	0.87	0.86	0.88
J_8	—	—	—	—	—	—	—	—	0.71	0.72	0.69	0.67
J_9	—	—	—	—	—	—	—	—	0.59	0.64	0.72	0.79

	20- story benchmark building											
	0.5 Hachinohe				1 Hachinohe				1.5 Hachinohe			
μ	3%	2%	1%	0.5%	3 %	2%	1%	0.5%	3%	2%	1%	0.5%
γ_{opt}	0.124	0.143	0.064	0.032	0.12	0.124	0.059	0.027	0.14	0.12	0.055	0.027
J_1	0.91	0.88	0.92	0.94	0.91	0.89	0.92	0.94	0.92	0.92	0.95	0.95
J_2	0.70	0.75	0.80	0.83	0.69	0.75	0.81	0.84	0.79	0.82	0.88	0.90
J_7	0.91	0.93	0.96	0.97	0.91	0.93	0.96	0.97	0.87	0.90	0.94	0.96
J_8	—	—	—	—	—	—	—	—	0.34	0.44	0.65	0.75
J_9	—	—	—	—	—	—	—	—	0.70	0.74	0.84	0.88

	9- story benchmark building											
	0.5 El Centro				1 El Centro				1.5 El Centro			
μ	3%	2%	1%	0.5%	3%	2%	1%	0.5%	3%	2%	1%	0.5%
γ_{opt}	0.05	0.028	0.010	0.004	0.054	0.041	0.017	0.006	0.028	0.022	0.017	0.007
J_1	0.94	0.92	0.89	0.88	0.91	0.93	0.97	0.96	0.91	0.88	0.93	0.97
J_2	0.71	0.73	0.75	0.77	0.73	0.78	0.76	0.80	0.81	0.80	0.90	0.83
J_7	0.89	0.89	0.91	0.91	0.91	0.93	0.96	0.95	0.75	0.83	0.91	0.94
J_8	—	—	—	—	0.79	0.78	0.89	0.90	1.04	0.81	0.85	0.87
J_9	—	—	—	—	0.84	0.90	0.94	0.92	1.04	0.96	1.01	1.00

	9- story benchmark building											
	0.5 Hachinohe				1 Hachinohe				1.5 Hachinohe			
μ	3%	2%	1%	0.5%	3%	2%	1%	0.5%	3%	2%	1%	0.5%
γ_{opt}	0.050	0.039	0.017	0.004	0.046	0.032	0.011	0.008	0.039	0.021	0.011	0.005
J_1	0.94	0.93	0.95	0.94	0.95	0.94	0.95	0.95	0.98	0.95	0.91	0.89
J_2	0.82	0.86	0.88	0.82	0.82	0.81	0.82	0.83	0.79	0.82	0.85	0.87
J_7	0.94	0.93	0.95	0.95	0.91	0.90	0.92	0.93	1.02	1.00	1.00	0.98
J_8	—	—	—	—	1.04	0.89	0.78	0.79	1.64	1.38	1.11	1.00
J_9	—	—	—	—	0.96	0.96	0.80	0.75	0.99	0.92	0.85	0.82

given the inappropriate increase in mass of the last floor and the high space occupied by liquid dampers at high mass ratios. Since liquid dampers are a special type of mass dampers, this trend is also seen in Elias et al. [31] study on control of a 20-story benchmark structure with a TMD for most earthquakes. According to Elias et al. [31], this is due to the use of a damper to control only the first mode of the structure and concentration of mass on one floor. However, this trend is inverse in the case for shorter 9-story benchmark structure in most cases, so that the maximum drift increases with decreasing mass ratio.

By investigation of the maximum acceleration criterion (J_2), it is found that the best performance of MTLD yielded 38% reduction for the 20-story structure under the El Centro earthquake and 29% reduction for the 9-story structure under the 0.5 El Centro earthquake. Contrary to the maximum drift

Table 3. Performance criteria responses of the 9- and 20-story benchmark structures with MTLD under near-field earthquakes for mass ratios of 0.5, 1, 2, and 3%.

20- story benchmark building							
0.5 Northridge				**1 Northridge**			
μ	**3%**	**2%**	**1%**	**0.5%**	**3%**	**2%**	**1%**	**0.5%**
γ_{opt}	0.048	0.034	0.017	0.008	0.303	0.381	0.186	0.089
J_1	1.10	1.06	1.00	0.98	0.95	0.93	0.94	0.95
J_2	0.79	0.84	0.89	0.92	0.77	0.78	0.85	0.89
J_7	0.97	0.92	0.90	0.93	0.96	0.94	0.95	0.95
J_8	1.31	0.93	0.82	0.77	1.48	1.18	0.92	0.88
J_9	0.81	0.85	0.85	0.91	0.91	0.93	0.96	0.97

20- story benchmark building							
0.5 Kobe				**1 Kobe**			
μ	**3%**	**2%**	**1%**	**0.5%**	**3%**	**2%**	**1%**	**0.5%**
γ_{opt}	0.112	0.03	0.016	0.008	0.049	0.031	0.015	0.008
J_1	1.02	0.98	0.95	0.94	0.92	0.87	0.91	0.91
J_2	0.68	0.74	0.79	0.81	0.87	0.87	0.89	0.91
J_7	0.70	0.75	0.86	0.91	1.03	0.94	0.98	1.00
J_8	1.64	1.03	0.63	0.57	1.29	1.11	0.93	0.83
J_9	0.79	0.89	0.84	0.82	0.90	0.93	0.94	0.96

9- story benchmark building							
0.5 Northridge				**1 Northridge**			
μ	**3%**	**2%**	**1%**	**0.5%**	**3%**	**2%**	**1%**	**0.5%**
γ_{opt}	0.039	0.022	0.014	*	0.030	0.019	0.009	0.004
J_1	0.94	0.93	0.97	0.98	1.06	1.01	0.96	0.97
J_2	0.78	0.80	0.84	0.97	0.89	0.88	0.87	0.94
J_7	0.86	0.90	0.93	0.97	1.02	0.99	0.98	0.99
J_8	0.90	0.94	0.97	0.99	0.88	0.92	0.95	0.94
J_9	0.92	0.92	0.94	1.00	1.03	1.03	0.95	0.95

9- story benchmark building							
0.5 Kobe				**1 Kobe**			
μ	**3%**	**2%**	**1%**	**0.5%**	**3%**	**2%**	**1%**	**0.5%**
γ_{opt}	0.017	0.011	0.007	0.003	0.017	0.012	0.010	0.006
J_1	0.82	0.83	0.84	0.85	0.86	0.87	0.91	0.92
J_2	0.83	0.87	0.90	0.92	0.92	0.93	0.94	0.94
J_7	0.80	0.80	0.80	0.80	0.87	0.89	0.92	0.94
J_8	0.52	0.52	0.51	0.52	0.71	0.74	0.74	0.74
J_9	0.92	0.92	0.92	0.92	1.00	1.00	1.00	1.00

*Very high values of $\frac{k_\theta}{k_s l^2}$ (same TLD).

ratio criterion, the maximum acceleration criterion is increased in most cases by decreasing the mass ratio.

After the maximum drift criterion (J_1), the ductility criterion (J_7) is one of the most important performance criteria, which is related to the evaluation of structural damage. Examination of Tables 2 and 3 shows that the ductility criterion is improved in almost all cases for benchmark structures controlled by MTLD. The highest J_7 criterion reduction for 9 and 20-story structures under far-field earthquakes was 25% (1.5 El Centro), 15% (El Centro), and under near-field earthquakes was 20% (0.5 Kobe) and 30% (0.5 Kobe), respectively.

The next criterion in the discussion of structural damage is the criterion of maximum dissipated energy at the end of members (J_8). The highest reduction of

Table 4. The mean responses of the five performance criteria in different mass ratios for near and far-field earthquakes for both benchmark structures.

	20- story benchmark building											
	Average for far-field historical records				Average for near-field historical records				Average for both kind historical records			
μ	3%	2%	1%	0.5%	3%	2%	1%	0.5%	3%	2%	1%	0.5%
J_1	0.91	0.90	0.91	0.91	1.00	0.96	0.95	0.95	0.946	0.924	0.926	0.926
J_2	0.68	0.82	0.79	0.82	0.78	0.81	0.86	0.88	0.720	0.816	0.818	0.844
J_7	0.88	0.90	0.91	0.93	0.92	0.89	0.92	0.95	0.896	0.896	0.914	0.938
J_8	0.53	0.58	0.67	0.71	1.43	1.06	0.83	0.76	0.890	0.772	0.734	0.730
J_9	0.65	0.69	0.87	0.84	0.85	0.90	0.90	0.92	0.730	0.774	0.828	0.872
	9- story benchmark building											
	Average for far-field historical records				Average for near-field historical records				Average for both kind historical records			
μ	3%	2%	1%	0.5%	3%	2%	1%	0.5%	3%	2%	1%	0.5%
J_1	0.94	0.93	0.93	0.93	0.92	0.91	0.92	0.93	0.932	0.922	0.926	0.930
J_2	0.78	0.80	0.83	0.82	0.86	0.87	0.89	0.94	0.812	0.828	0.854	0.868
J_7	0.90	0.91	0.94	0.94	0.89	0.90	0.91	0.93	0.896	0.906	0.928	0.936
J_8	1.13	0.97	0.91	0.89	0.75	0.78	0.79	0.80	0.978	0.894	0.862	0.854
J_9	0.96	0.94	0.90	0.87	0.97	0.97	0.95	0.97	0.964	0.952	0.920	0.910

Table 5. Mean decrease of performance criteria responses for MTLD-controlled benchmark structures compared to traditional TLD-controlled ones.

20- story benchmark building				
μ	3%	2%	1%	0.5%
Reduction J_1 (%)	5.5	5.3	4.1	3.0
Reduction J_2 (%)	2.6	2.8	3.1	3.0
Reduction J_7 (%)	1.0	0.4	0.3	0.7
Reduction J_8 (%)	19.8	20.3	16.0	9.3
Reduction J_9 (%)	1.2	−0.8	−0.7	−1.0
9- story benchmark building				
μ	3%	2%	1%	0.5%
Reduction J_1 (%)	9.7	8.4	6.3	6.1
Reduction J_2 (%)	8.1	9.2	10.1	9.8
Reduction J_7 (%)	5.9	6.2	5.5	5.3
Reduction J_8 (%)	35.5	22.1	14.8	14.4
Reduction J_9 (%)	5.8	6.8	8.0	8.6

the J_8 criterion for the 20-story structure was under the far-field 1.5 Hachinohe earthquake being equal to 66%. For the 9-story structure, the differences in the effect of MTLD on the J_8 criterion are large. The ratio of the number of plastic hinges formed in the control structure to the uncontrolled structure (J_9) is the next important criterion in the discussion of structural damage. The highest reduction of the J_9 criterion for 20-story structures under far-field (1.5 El Centro) and near-field (0.5 Kobe) earthquakes was 41% and

21%, respectively. In the 9-story structure, the largest reduction in the number of plastic hinges occurred under the Hachinohe far-field earthquake by 25% and under the near-field 0.5 Northridge earthquake by 8%.

According to Table 4, it can be concluded that the highest decrease in maximum drift occurred for both controlled benchmark structures at 2% mass ratio and is similar at about 8%. According to Sections 3 and 4.3, the low inherent damping of MTLD and miss-tuning under high-intensity and near-field earthquakes, can be the reasons for not achieving better responses. The average reduction in maximum acceleration was between 13-28% for the two benchmark structures. A brief look at the columns for the mean responses under both earthquakes in Table 4 shows that the greatest effect of MTLD for both structures was on the maximum acceleration criterion. This suggests that MTLD is better suited to reduce the maximum acceleration of structures than to reduce the maximum drift, and may therefore be appropriate to reduce the effect of wind on high-rise structures.

Summarizing the mean responses of all 5 criteria, shows that under far-field earthquakes the effect of MTLD on the 20-story structure was greater than the 9-story structure. However, under near-field earthquakes, the performance of the 9 and 20-story controlled structures are almost similar. In general, the greatest effect of MTLD is on the reduction of maximum acceleration of structures (J_2) as well as important criteria in the structural damage included maximum dissipation energy (J_8), number of plastic

hinges (J_9) and ductility (J_7), respectively. Since the performance criteria responses in the two benchmark structures is dependent to the mass ratio, it is necessary to determine the optimal mass ratio. Therefore, by examining the mean of the criterion responses in Table 4, it can be seen that an average mass ratio of 2% can be considered as the optimal mass ratio for both structures.

The comparison between the drift responses from the MTLD and traditional TLD on both benchmark structures under all earthquakes is shown in Figure 11. According to this figure, the largest difference between the effect of MTLD and traditional TLD on the J_1 criterion was 12% for 20-story structure and 18% for 9-story structure under 1.5 Hachinohe and 0.5 Kobe earthquakes at 3% mass ratio, respectively. In Figure 11, it is shown that at worst, the performance of the MTLD is the same as the traditional TLD. For example, we can point out the control of the 9-story structure under the 0.5 Northridge earthquake, in which the best performance of MTLD was the same as the traditional TLD.

In Table 5, the mean decreases in the responses of the five most important performance criteria, are shown for different mass ratios for MTLD-controlled benchmark structures compared to traditional TLD-controlled ones. As can be seen, the increase in the effect of MTLD over traditional TLD on the reduction of mean maximum drift in the 9-story structure was greater than that of the 20-story structure. In fact, the difference between the performances of the two types of dampers on the 9-story structure is greater than the 20-story structure in all five criteria. For the 20-story structure, the greatest improvement in MTLD performance over the traditional TLD is on the J_8 criterion (up to 20%) and next on the J_1 criterion (up to 5.5%). For the 9-story structure, the performance improvement of MTLD over traditional TLD was evident in more criteria, with the highest being attributed to J_8 (up to 35.5%), J_2 (up to 10%) and J_1 (up to 9.7%) criteria.

4.5. MTLD range of effect
In Table 6, the maximum and mean values of γ for which MTLD is converted to the traditional TLD, are shown for each benchmark structure at different mass
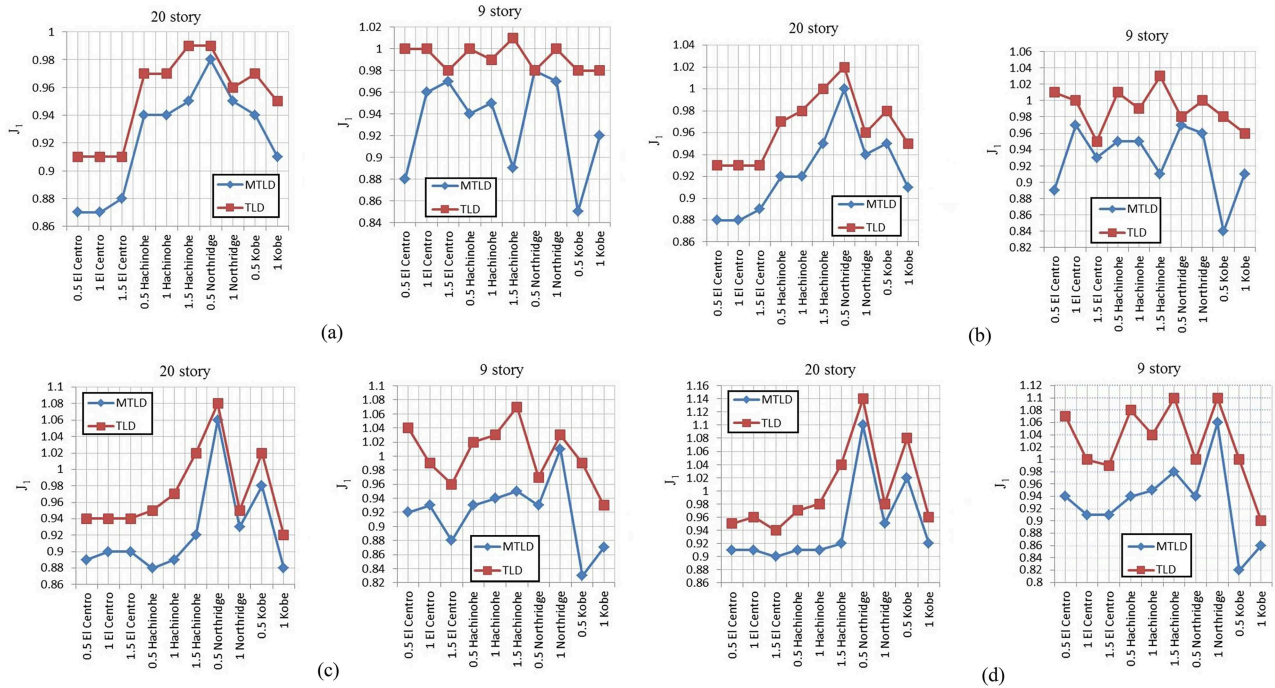
Figure 11. Comparison between the drift responses from the MTLD and traditional TLD on both 9- and 20-story benchmark structures under all earthquakes for mass ratio of (a) 0.5%, (b) 1%, (c) 2%, and (d) 3%.

Table 6. Maximum and mean values of the dimensionless rotational stiffness parameter γ, for which MTLD is converted to the traditional TLD.

	3%		2%		1%		0.5%	
μ	Max	Avg	Max	Avg	Max	Avg	Max	Avg
γ_{20str}	0.55	0.40	0.50	0.40	0.38	0.23	0.28	0.18
γ_{9str}	0.45	0.35	0.40	0.30	0.35	0.20	0.20	0.15

Table 7. Minimum and mean values of dimensionless rotational stiffness parameter γ, for which the effect of MTLD on benchmark structures is vanished.

μ	3%		2%		1%		0.5%	
	Min	Avg	Min	Avg	Min	Avg	Min	Avg
γ_{20str}	0.028	0.043	0.020	0.028	0.008	0.013	0.003	0.007
γ_{9str}	0.006	0.013	0.005	0.007	0.003	0.004	0.001	0.002

ratios. This occurs when the stiffness of the MTLD rotational spring for the parameter γ is high enough to lower the damper tank rotation to near zero. The results of Table 6 show that the conversion limit of MTLD to traditional TLD was almost similar to the value suggested by Samanta and Banerji [22] ($\gamma = 0.5$), and the maximum occurred at $\gamma = 0.55$.

The minimum and mean values of γ for which the effect of MTLD on benchmark structures is eliminated, are presented in Table 7 for different mass ratios. The MTLD effect disappears when the stiffness of the rotational spring is so low that its rotation is greatly increased and the performance of the controlled benchmark structure approaches the uncontrolled benchmark structure. Samantha and Banerji [22] have proposed the elimination limit of the MTLD effect for a SDOF structure for $\gamma = 0.05$. But the results in Table 7 show that this limit for multiple-degree of freedom benchmark structures can be well below 0.05. As shown in Table 7, as the mass ratio decreases and the number of floors is reduced (reduction of the number of degrees of freedom), the γ parameter value is also decreased.

5. Summary and conclusion

In this study, the performance of Modified Tuned Liquid Damper (MTLD) is evaluated to control the seismic response of 9 and 20-story benchmark structures with nonlinear behavior. Since the main focus has been on the maximum drift reduction (J_1) of the structure, in each case the dimensionless rotational stiffness parameter (γ) has been adjusted to reach highest reduction in maximum drift response. Evaluations show that MTLD performance depends on the type of structure and earthquake. However, the average results indicate that the use of MTLD reduced the structural responses (J_1 and J_2) and nonlinear performance criteria (J_7–J_9) of both benchmark structures for all mass ratios. The most important results extracted from the numerical study are as follows: the first it can be said that MTLD is more reliable for effectively reducing the acceleration response than structural drift response and may be suitable for reducing the wind effect on tall structures. Second, Numerical investigation of the nonlinear performance criteria of benchmark structures shows that besides reduction of maximum acceleration, MTLD has the greatest effect on reducing the damage criteria of the structures. Third, although there is no clear

and consistent trend between mass ratio variations and its effect on performance criteria, it can still be claimed that the performance of MTLD at 2% mass ratio was better than other mass ratios. The fourth, performance of MTLD was evaluated and compared with Turned Liquid Damper (TLD), Comparison shows that the MTLD reduced the maximum drift of 9 and 20-story structures by 18% and 12% more than the TLD, respectively. In the worst case, performance of MTLD was similar to TLD. Also in other criteria the MTLD performance was usually better than the TLD. And fifth, the MTLD effective range varies depending on the type of the structure and mass ratio. The MTLD effective range for 9 and 20-story benchmark structures can be considered as approximately $0.001 < \gamma < 0.55$.

Conflicts of interest: The author(s) declared no potential conflicts of interest with respect to the research, authorship, and/or publication of this article.

References

1. Fujino, Y., Sun, L., Pacheco, B.M., et al. "Tuned liquid damper (TLD) for suppressing horizontal motion of structures", *Journal of Engineering Mechanics*, **118**(10), pp. 2017–2030 (1992). https://doi.org/10.1061/(ASCE)0733-9399(1992)118:10(2017)

2. Horikawa, K. "Coastal engineering: an introduction to ocean engineering", Publ. by: University of Tokyo Press (1978).

3. Kim, Y.M., You, K.P., Cho, J.E., et al. "The vibration performance experiment of tuned liquid damper and tuned liquid column damper", *Journal of Mechanical Science and Technology*, **20**(6), pp. 795–805 (2006). https://doi.org/10.1007/BF02915943

4. Bauer, H.F. "Oscillations of immiscible liquids in a rectangular container: a new damper for excited structures", *Journal of Sound and Vibration*, **93**(1), pp. 117–133 (1984). https://doi.org/10.1016/0022-460X(84)90354-7

5. Kareem, A. and Sun, W.J. "Stochastic response of structures with fluid-containing appendages", *Journal of Sound and Vibration*, **119**(3), pp. 389–408 (1987). https://doi.org/10.1016/0022-460X(87)90405-6

6. Shimizu, T. and Hayama, S. "Nonlinear responsed of sloshing based on the shallow water wave theory: Vibration, control engineering, engineering for industry", *JSME International Journal*, **30**(263), pp. 806–813 (1987). https://doi.org/10.1299/jsme1987.30.806

7. Sun, L.M., Fujino, Y., Pacheco, B.M., et al. "Modelling of tuned liquid damper (TLD)", *Journal of Wind Engineering and Industrial Aerodynamics*, **43**(1–3), pp. 1883–1894 (1992). https://doi.org/10.1016/0167-6105(92)90609-E

8. Koh, C.G., Mahatma, S., and Wang, C.M. "Theoretical and experimental studies on rectangular liquid dampers under arbitrary excitations", *Earthquake Engineering and Structural Dynamics*, **23**(1), pp. 17–31 (1994). https://doi.org/10.1002/eqe.4290230103

9. Sun, L.M., Fujino, Y., and Koga, K. "A model of tuned liquid damper for suppressing pitching motions of structures", *Earthquake Engineering and Structural Dynamics*, **24**(5), pp. 625–636 (1995). https://doi.org/10.1002/eqe.4290240502

10. Banerji, P., Murudi, M., Shah, A.H., et al. "Tuned liquid dampers for controlling earthquake response of structures", *Earthquake Engineering and Structural Dynamics*, **29**(5), pp. 587–602 (2000). https://doi.org/10.1002/(SICI)1096-9845(200005)29:5¡587::AID-EQE926¿3.0.CO;2-I

11. Lu, M.L., Popplewell, N., Shah, A.H., et al. "Nutation damper undergoing a coupled motion", *Modal Analysis*, **10**(9), pp. 1313–1334 (2004). https://doi.org/10.1177/1077546304042045

12. Samanta, A. and Banerji, P. "Efficient numerical schemes to analyse earthquake response of structures with tuned liquid dampers", *Symposium on Earthquake Engineering* (2006, January).

13. Soliman, I. "Passive and semi-active structure-multiple tuned liquid damper systems", PhD Thesis, University of Western Ontario (2012).

14. Shoaei, P. and Oromi, H.T. "A combined control strategy using tuned liquid dampers to reduce displacement demands of base-isolated structures: a probabilistic approach", *Frontiers of Structural and Civil Engineering*, **13**(4), pp. 890–903 (2019). https://doi.org/10.1007/s11709-019-0524-8

15. Shin, J.H., Kwak, M.K., Kim, S.M., et al. "Vibration control of multi-story building structure by hybrid control using tuned liquid damper and active mass damper", *Journal of Mechanical Science and Technology*, **34**(12), pp. 5005–5015 (2020). https://doi.org/10.1007/s12206-020-1105-4

16. Enayati, H. and Zahrai, S.M. "A variably baffled tuned liquid damper to reduce seismic response of a five-storey building", *Proceedings of the Institution of Civil Engineers-Structures and Buildings*, **171**(4), pp. 306–315 (2018). https://doi.org/10.1680/jstbu.16.00034

17. McNamara, K.P., Awad, B.N., Tait, M.J., et al. "Incompressible smoothed particle hydrodynamics model of a rectangular tuned liquid damper containing screens", *Journal of Fluids and Structures*, **103**, 103295 (2021). https://doi.org/10.1016/j.jfluidstructs.2021.103295

18. Zhang, Z. "Numerical and experimental investigations of the sloshing modal properties of sloped-bottom tuned liquid dampers for structural vibration control", *Engineering Structures*, **204**, p. 110042 (2020). https://doi.org/10.1016/j.engstruct.2019.110042

19. Pandit, A.R. and Biswal, K.C. "Seismic control of multi degree of freedom structure outfitted with sloped bottom tuned liquid damper", In *Structures*, **25**, pp. 229–240, Elsevier (2020). https://doi.org/10.1016/j.istruc.2020.03.009

20. Konar, T. and Ghosh, A. "Development of a novel tuned liquid damper with floating base for converting deep tanks into effective vibration control devices", *Advances in Structural Engineering*, **24**(2), pp. 401–407 (2021). https://doi.org/10.1177/1369433220953539

21. Ruiz, R., Taflanidis, A.A., Lopez-Garcia, D., et al. "Life-cycle based design of mass dampers for the Chilean region and its application for the evaluation of the effectiveness of tuned liquid dampers with floating roof", *Bulletin of Earthquake Engineering*, **14**(3), pp. 943–970 (2016). https://doi.org/10.1007/s10518-015-9860-9

22. Samanta, A. and Banerji, P. "Structural vibration control using modified tuned liquid dampers", *The IES Journal Part A: Civil & Structural Engineering*, **3**(1), pp. 14–27 (2010). https://doi.org/10.1080/19373260903425410

23. Chang, Y., Noormohamed, A., and Mercan, O. "Analytical and experimental investigations of Modified Tuned Liquid Dampers (MTLDs)", *Journal of Sound and Vibration*, **428**, pp. 179–194 (2018). https://doi.org/10.1016/j.jsv.2018.04.039

24. Kamgar, R., Gholami, F., Sanayei, H.R.Z., et al. "Modified tuned liquid dampers for seismic protection of buildings considering soil-tructure interaction effects", *Iranian Journal of Science and Technology, Transactions of Civil Engineering*, pp. 1–16 (2019). https://doi.org/10.1007/s40996-019-00302-x

25. Wang, J.T., Gui, Y., Zhu, F., et al. "Real-time hybrid simulation of multi-story structures installed with tuned liquid damper", *Structural Control and Health Monitoring*, **23**(7), pp. 1015–1031 (2016). https://doi.org/10.1002/stc.1822

26. Eswaran, M., Athul, S., Niraj, P., et al. "Tuned liquid dampers for multi-storey structure: numerical simulation using a partitioned FSI algorithm and experimental validation", *Sādhanā*, **42**(4), pp. 449–465 (2017). https://doi.org/10.1007/s12046-017-0614-z

27. Tuong, B.P.D., Huynh, P.D., Bui, T.T., et al. "Numerical analysis of the dynamic responses of multistory

structures equipped with tuned liquid dampers considering fluid-structure interactions", *Open Construction and Building Technology Journal*, **13**(1), pp. 289–300 (2019).
https://doi.org/10.2174/1874836801913010289

28. Ohtori, Y., Christenson, R.E., Spencer Jr, B.F., et al. "Benchmark control problems for seismically excited nonlinear buildings", *Journal of Engineering Mechanics*, **130**(4), pp. 366–385 (2004).
https://doi.org/10.1061/(ASCE)0733-9399(2004)130:4(366)

29. Cunge, J. "Practical aspects of computational river hydraulics", *Pitman Publishing Ltd*, London, (17 CUN), 420 (1980).

30. Stoker, J.J., *Water Waves: The Mathematical Theory with Applications*, **36**, John Wiley and Sons (1992).

31. Elias, S., Matsagar, V., and Datta, T.K. "Distributed tuned mass dampers for multi-mode control of benchmark building under seismic excitations", *Journal of*

Earthquake Engineering, pp. 1–36 (2017).
https://doi.org/10.1080/13632469.2017.1351407

Biographies

Amir Hosein Daneshmand is a PhD student of Structural Engineering at Ferdowsi University of Mashhad (FUM). He received his MSc degree from Shahid Bahonar University of Kerman in 2015. His research interests are crack analysis and structural control.

Abbas Karamodin is an Associate Professor of Civil Engineering at Ferdowsi University of Mashhad. He received his PhD from Ferdowsi University of Mashhad. His studies cover a wide range of topics in the structural and earthquakes engineering including structural control, performance-based engineering, and fire engineering.